JOURNAL OF VISUAL COMMUNICATION AND IMAGE REPRESENTATION
Vol. 5, No. 1, March, pp. 29–40, 1994

Morphological Image Coding Based on a Geometric Sampling Theorem and a Modified Skeleton Representation*

GUILLERMO SAPIRO AND DAVID MALAH

Technion—Israel Institute of Technology, Department of Electrical Engineering, Haifa 32000, Israel

Received May 8, 1991; accepted October 21, 1992

A new approach for gray-level image coding using binary morphological operations on the image bit-planes is presented. This approach is based on a Geometric Sampling Theorem (GST), and on a modified morphological skeleton. The theorem, which is proved in this paper, states conditions for the reconstruction of the boundary of a continuous two level image from a unique subset of points of its skeleton representation. This set of points, referred to as essential points, is found to play an important role in the skeleton representation of discrete binary images as well. The modified morphological skeleton (MMS) uses an exponentially increasing in size structuring element. The computational advantage of this representation was previously reported. A new approach to its development is presented here, and its advantage in image coding is demonstrated. The coding scheme consists of the following steps: First, the image is preprocessed by an error-diffusion technique in order to reduce the number of bit-planes from 8 to 4 without significant quality degradation. The pixel values are subsequently converted to Gray-code. The bit-planes are represented by the MMS. Redundancy in this representation is reduced using an algorithm motivated by the GST. These reduced modified morphological skeletons are coded with an entropy coding scheme particularly devised for efficient skeleton coding. The possibility of the introduction of geometric errors to reduce the bit-rate is also discussed. Compression ratios of up to 11:1 were obtained for satellite images.

I. INTRODUCTION

Medial axis and skeleton representations have received much attention, both in theoretical [1–4] and in practical aspects [5]. This paper concentrates on reconstruction properties of the skeleton, and presents a *Geometric Sampling Theorem* (*GST*) [6]. The theorem deals with the representation, via a skeleton subset, of sets in the continuous two dimensional space R^2. In the second part of the paper, a new approach to gray-level image coding is presented [7], which is based on the GST and on a *modified* morphological skeleton which uses an *exponentially increasing in size* structuring element [8] instead of the linearly increasing in size element that is commonly used [5, 8].

The GST states conditions for the reconstruction of the boundary of *a continuous* two level image (i.e., a set of R^2) from a *unique* subset of points of its skeleton representation. These points are called here *essential points*. The analogy between this theorem and the classical Sampling Theorem is given as well. In the case of discrete binary images (i.e., sets of Z^2), we found that the essential points of the discrete skeleton convey most of the information required for reconstruction. Based on this fact, we develop an algorithm for efficient computation of the *minimal skeleton* [5] of discrete binary images (i.e., a subset of the skeleton whose points are sufficient for exact reconstruction, and which satisfies the condition that the image cannot be recovered from any subset of it).

Recently, Maragos and Schafer [5] presented a scheme for binary image coding which exploits the geometry of these images via morphological skeleton representation. In [8], Schonfeld and Goutsias presented a *geometric-step morphlogical skeleton* (*GSMS*), which results in an *exponentially increasing in size* structuring element. They proved that, when this skeleton is implemented on a pipelined morphological processor (*PMP*), its computational complexity is less than that in [5]. We present here a new approach for developing what we denote as a *modified* morphological skeleton, which was found to be a special case of the GSMS. This approach was motivated by the fact that when fewer skeleton subsets are obtained in the image representation, the compression ratio can be increased (unlike the computational motivation in [8]).

The approach used for gray-level image coding is as follows: The image is first pre-processed by an error diffusion technique [9] in order to reduce the number of bit planes from 8 to 4, without significant quality degradation. The pixel values are subsequently represented in Gray-code in order to obtain more uniform bit-planes. These bit-planes are represented each by means of a *modified* morphological skeleton, and redundancy in this representation is reduced using an algorithm which is based on the GST. These skeletons, which are sparse

* This article was originally scheduled to appear in the Mathematical Morphology special issue of *Journal of Visual Communication and Image Representation* (Vol. 3, No. 2, June 1992).

1047-3203/94 $6.00

representations of the bit-planes, are coded with a combination of different entropy coders particularly devised for efficient skeleton coding. These include Huffman coding of the number of consecutive lines having no skeleton points, and run-length followed by Huffman coding for the remaining lines. Geometric errors in the bit-planes can also be introduced for bit-rate reduction. In such a case, postprocessing operations for quality enhancement of the image, such as random filling of undefined areas in the partially reconstructed bit-planes, are also suggested.

The remainder of this paper is organized as follows: Basic concepts of mathematical morphology are given in Section II. Section III introduces the skeleton of a continuous image and presents the GST. Section IV presents the morphological skeleton of a discrete image and describes the *modified morphological skeleton*. In Section V, description of the coding algorithm is given. Experimental results are presented in Section VI, and finally a summary and conclusions in Section VII.

II. CONCEPTS OF MATHEMATICAL MORPHOLOGY

Let R be the set of real numbers, Z the set of integers, and E the Euclidean space R^2 or Z^2. Upper case letters stand for subsets of E, and lower case letters for elements or points of E. The simplest morphological transformations are based on the Minkowski set addition and set subtraction [1, 10]. The morphological *dilation*, derived from the Minkowski set addition, is defined [1, 10, 11] as

$$A \oplus B = \{a + b: a \in A, b \in B\} = \bigcup_{b \in B} A_b, \quad (1)$$

where $X_y = \{x + y: x \in X\}$ (*translate* of X by the vector y). B is called the *structuring element*. In the definitions presented here (and in Section IV), B is assumed to be symmetric [1, 10, 11] (see also Section V.B).

From the Minkowski set subtraction, the second basic morphological transformation, *erosion*, is defined [1, 10, 11] (different definitions can be found in the literature, but in the case of symmetric structuring elements, all those definitions are equivalent) as

$$A \ominus B = (A^c \oplus B)^c = \bigcap_{b \in B} A_b, \quad (2)$$

where X^c stands for set complement. In other words, the erosion of A is the locus of the points a for which $B_a \subseteq A$.

From the combination of these dual morphological operations, a new pair of dual morphological transformations is derived: *opening* and *closing* [1, 10, 11]. Opening is defined as

$$A \circ B = (A \ominus B) \oplus B \quad (3)$$

and closing as

$$A \bullet B = (A \oplus B) \ominus B = (A^c \circ B)^c. \quad (4)$$

It can be shown that

$$A \circ B = \{x \in A: \text{for some } y,\ x \in B_y \subseteq A\} = \bigcup_{\{y | B_y \subseteq A\}} B_y. \quad (5)$$

That means that the opening of A by B is the union of all translations of B that are contained in A (geometric characterization of the closing operation is immediate from its duality with opening). Opening is the *morphological smoothing* of the set A (every place where the given structuring element does not fit the set is eliminated). In the same way, closing is the morphological smoothing of the set complement A^c. For properties of these operations and their extensions to sets of R^N or Z^N and to multivalued functions, see [1, 10, 11].

III. MORPHOLOGICAL SKELETON AND A GEOMETRIC SAMPLING THEOREM

A. *Skeleton of Continuous Images*

Let X be a closed set in R^2. The curvature $\kappa(p)$ at a point p of the boundary ∂X of the set X is defined as the inverse of the radius of the osculating disk tangent to ∂X at p [12]. We assume that the Convex Hull of X^C is equal to R^2 (a necessary condition for the exact reconstruction of X [1–4]) and that $\kappa(\cdot)$ of ∂X is well defined everywhere, except at a finite number of points, where it may have only one-sided tangents. We denote these sets of boundary points by $\Gamma(X)$, $\Gamma(X) \subset \partial X$. The subset of points in $\Gamma(X)$ for which the correspondent interior angle is concave (e.g., the points b, f in Fig. 1) is denoted by $\xi(X)$.

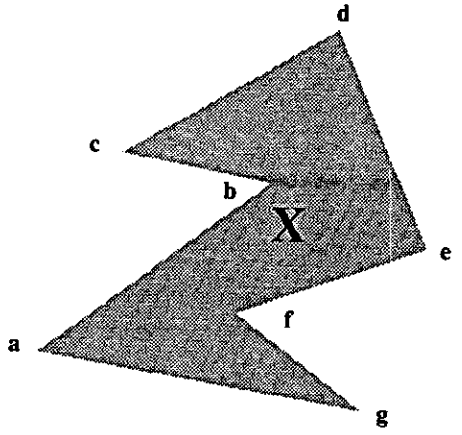

FIG. 1. A continuous set X with points which do not have well defined curvature: $\Gamma(X) = \{a, b, \ldots, g\}$, $\xi(X) = \{b, f\}$.

We also define $Y_\rho \triangleq X \circ \rho U$, where U is the unit disk in R^2.

Let $D(x, \rho)$ be a closed disk of center x and radius $\rho \geq 0$ (in a two dimensional Euclidean space). Then a maximal disk in X and the skeleton of X are defined as follows:

MAXIMAL DISK. A *maximal disk* $D(\psi, \rho_\psi)$ is one which is included in the object X, but not in any other disk in X.

SKELETON IN R^2: The *skeleton* $\Psi(X)$ of an object $X \subset R^2$ is defined as the family of centers of all maximal disks in X [1–4, 13].

Hence, if $\psi \in \Psi(X)$, then $D(\psi, \rho_\psi)$ denotes its corresponding maximal disk with radius ρ_ψ; i.e., ρ_ψ is the Euclidean distance from ψ to ∂X.

It is well known [1–4] that under the assumed conditions, X can be reconstructed from the set $\Psi(X)$ together with the set of radii ρ_ψ, i.e., from the *skeleton pairs* (ψ, ρ_ψ):

$$X = \bigcup_{\psi \in \Psi(X)} D(\psi, \rho_\psi), \tag{6}$$

B. A Geometric Sampling Theorem

Not all skeleton points are necessarily needed for exact reconstruction. We are interested in a set of points $\Psi_m(X) \subseteq \Psi(X)$, denoted as the *minimal skeleton* [5], which guarantees exact reconstruction of X, and which satisfies the condition that X cannot be recovered from any subset of $\Psi_m(X)$. Such a set exists, because in the worst case $\Psi_m(X) = \Psi(X)$. Similarly, we are interested in the minimal set for recovering ∂X.

For demonstration, Fig. 2 shows a set in R^2 with its skeleton. The skeleton of the set X is the closed segment $[a, b]$; i.e., $\Psi(X) = [a, b]$ (see [2, Chap. 11]). In this case, clearly, the two marked points $\{a, b\}$, together with their corresponding radii $\{\rho_a, \rho_b\}$, are sufficient for object reconstruction and constitute a minimal skeleton: $\Psi_m(X) = \{a, b\}$ and hence $\Psi_m(X) \subset \Psi(X)$.

Before proceeding, we also define the following:

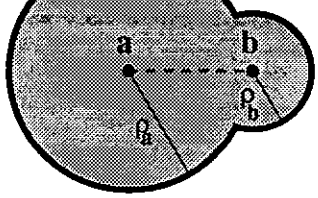

FIG. 2. Example of a skeleton (dashed line) and a minimal skeleton (points a, b): $\Psi_m(X) = \{a, b\}$.

ESSENTIAL POINT: A skeleton point s, $s \in \Psi(X)$, is an *essential point* if and only if there exists a point p in X such that the maximal disk $D(s, \rho_s)$ is the only one which contains it. I.e.,

$$s \in \Psi(X) \text{ is an essential point} \Leftrightarrow \begin{cases} \exists\, p \in X,\ p \in D(s, \rho_s): \\ \forall\, \psi \in \Psi(X),\ \psi \neq s \Rightarrow p \notin D(\psi, \rho_\psi). \end{cases} \tag{7}$$

Also, for any point $s \in \Gamma(X) \backslash \xi(X)$, s is essential with a maximal disk $D(s, \rho_s)$ of radius $\rho_s = 0$ (e.g., points a and d in Fig. 1).

MINIMAL RECONSTRUCTION. Let $S(X)$ be the unique set of essential points in X. Then X^* denotes the *minimal reconstruction* defined by

$$X^* \triangleq \bigcup_{s \in S(X)} D(s, \rho_s), \qquad X^* \subseteq X. \tag{8}$$

BOUNDARY ESSENTIAL POINT. Similarly, we say that a point $s \in \Psi(X)$ is a *boundary essential point* if and only if there exists a point p on ∂X (the boundary of X) such that the maximal disk $D(x, \rho_x)$ is the only one which contains it. I. e.,

$$s \in \Psi(X) \text{ is a boundary essential point} \Leftrightarrow \begin{cases} \exists\, p \in \partial X,\ p \in D(s, \rho_s): \\ \forall\, \psi \in \Psi(X),\ \psi \neq s \Rightarrow p \notin D(\psi, \rho_\psi). \end{cases} \tag{9}$$

The notion of essential points and the relation between $S(X)$ and $\Psi_m(X)$ are illustrated in Figs. 1 and 2 as follows:

In the case of the set in Fig. 2, the two marked points a, b are essential and hence $\Psi_m(X) = S(X)$. The points in the open segment (a, b) are in $\Psi(X)$ but not in $S(X)$.

In the set of Fig. 1, the points b and f are each covered by more than one maximal disk centered at nonessential skeleton points. Hence, $S(X)$ is not sufficient for the reconstruction of X, and $S(X) \subset \Psi_m(X)$.

The importance of essential points is evident from these examples and from the following theorems.

Lemma 1 gives the relation between the set of *essential points* $S(X)$, and the minimal skeleton $\Psi_m(X)$:

LEMMA 1. *All essential points are in* $\Psi_m(X)$.

Proof. This is a direct consequence from the definitions of the skeleton and the essential points, since the maximal disk corresponding to an essential point contributes at least one point which is not included in any other maximal disk in X.

Hence, we conclude that $S(X) \subseteq \Psi_m(X)$. ■

THEOREM 1. *$x \in X$ is a boundary essential point if and only if x is an essential point.*

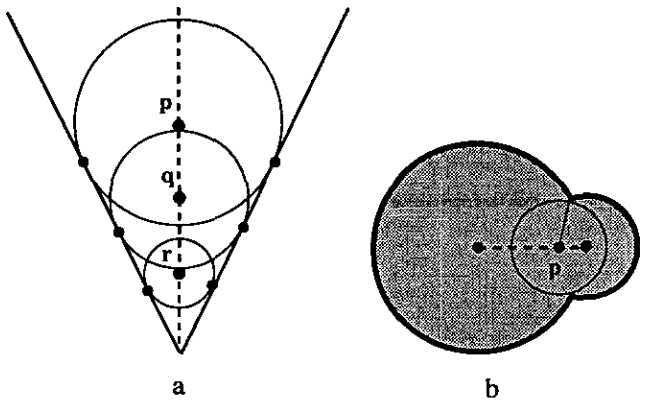

FIG. 3. Different types of skeleton points and the tangent points of their maximal disks with the boundary. (a) Maximal disks corresponding to essential points (p, q, r). (b) Maximal disk of a nonessential point (p).

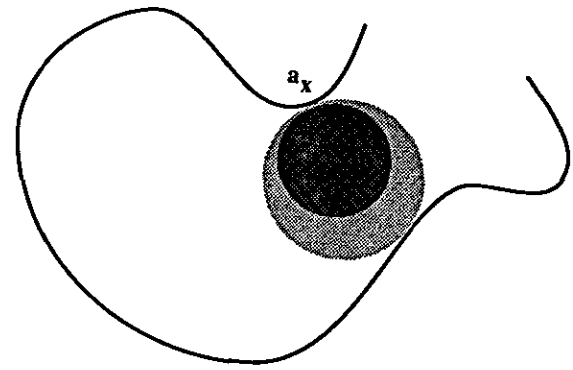

FIG. 4. Nested circles. Only the outer one corresponds to a maximal disk.

Proof. $\Rightarrow$ From the definitions, if x is boundary essential, then x is essential.

$\Leftarrow$ Given an essential point x, we have to prove that x is boundary essential. For all $z \in \Psi(X)$, $D(z, \rho_z) \cap \partial X \neq \emptyset$ (see marked points in Fig. 3). If $D(z, \rho_z)$, with $z \in \Psi(X)$ and $\rho_z > 0$, touches ∂X only at points with curvature *not* well defined, i.e., $D(z, \rho_z) \cap \partial X \subseteq \xi(X)$; then z cannot be an essential point (all the points of its maximal disk are covered by more than one maximal disk). Therefore, for any essential point $x \in \Psi(X)$, its corresponding maximal disk $D(x, \rho_x)$ touches the object boundary at least at one point a_x (see Fig. 4), such that $a_x \in D(x, \rho_x) \cap \partial X$ and $a_x \in \partial X \backslash \xi(X)$. If we prove that $D(x, \rho_x)$ is the only maximal disk which contributes to a_x, then x is also a boundary essential point.

Let us prove now that $D(x, \rho_x)$ is the only maximal disk which touches ∂X at a_x, when $\kappa(a_x)$ is well defined. We have to show that there is no other $y \in \Psi(X)$, $x \neq y$, such that $a_x \in D(y, \rho_y) \cap \partial X$. Suppose such a y does exist. Since the curvature $\kappa(a_x)$ is well defined, then both $D(x, \rho_x)$ and $D(y, \rho_y)$ are tangent to ∂X at a_x; and $x, y \in N_{a_x}$, where N_p stands for the normal to ∂X at a point $p \in \partial X$ with $\kappa(p)$ well defined. This means that $D(x, \rho_x)$ and $D(y, \rho_y)$ are nested disks (see Fig. 4), a contradiction to the hypothesis that they are maximal disks $(x, y \in \Psi(X))$. Then, $D(x, \rho_x)$ is the only maximal disk which contains $a_x \in \partial X$, and x is a boundary essential point. ■

The meaning of this theorem is that an essential skeleton point contributes to X if and only if it contributes to ∂X. Therefore, when looking for an essential point, only contributions of maximal disks to the set boundary need to be checked.

THEOREM 2 (The Geometric Sampling Theorem). *Let X be a set in R^2, with boundary ∂X, and minimal reconstruction X^*. Let Y_ρ be the set obtained by opening X with a disk of radius ρ. Then*

(a) X^* covers the whole boundary (∂X) of X, except for a finite number of points.

(b) The subset of $S(X)$ containing essential points with corresponding radii $r \geq \rho$, is sufficient for the reconstruction of the whole boundary of Y_ρ, except for a finite number of points (these points are the same as in the first part of the theorem).

Proof. (a) Any boundary point $a_x \in \partial X$ belongs at least to one maximal disk $D(x, \rho_x)$ (Eq. (6)), $x \in \Psi(X)$. In the proof of Theorem 1 we showed that if $\kappa(a_x)$ is well defined, then x is an essential point (or a boundary essential point). Therefore, X^* covers at least all the boundary points with well defined curvature, i.e., $\partial X \backslash \xi(X)$, and the number of uncovered points is at most $\# \xi(X) < \infty$.

For coverage of the uncovered points (a subset of $\xi(X)$), we have to add to the reconstruction set, skeleton points with corresponding maximal disks touching ∂X just at points in $\xi(X)$. Each one of these maximal disks touches ∂X at least at two points; therefore the number of skeleton points that must be added is less than or equal to $[\# \xi(X)]/2$.

(b) This is a direct consequence from the first part of the theorem and from the fact that $Y_\rho = \bigcup_{\psi \in \Psi(X), \rho_\psi \geq \rho} D(\psi, \rho_\psi)$ [1,2]. ■

From the above two theorems we see the importance of the unique set $S(X)$ for the reconstruction of X, since each essential point contributes to ∂X and almost all of ∂X is covered by the maximal disks of $S(X)$. By the second part of Theorem 2 one is motivated to denote the morphological operation $X \circ \rho B$ as *a geometric low pass filter,* in analogy to the filter used in classical signal processing, with bandwidth being replaced here by the inverse of the radius of the maximal disk [2, 5, 14].

As stated in Theorem 2, when X is opened by ρB

(yielding Y_ρ), parts of the skeleton are eliminated. This means that fewer data need to be coded for reconstruction of the smoothed set Y_ρ. For non-error-free compression tasks, it is very important to estimate this reduction in the data needed for representation as a function of ρ (which determines the set degradation). Related to this issue, a lower bound on the length of skeleton arcs eliminated by the opening operation is given for continuous sets in the Appendix. For discrete sets, simulation results are given in Section VI.

Extensions of the theorems, and an extended analysis of the analogy between these theorems and the classical Sampling Theorem, are given in [14].

IV. MORPHOLOGICAL SKELETONS OF DISCRETE IMAGES

A. Basic Morphological Skeleton

The skeleton $SK^B(X)$ of a *discrete* set X (a subset in Z^2) can be defined in a way similar to the skeleton of a continuous set [1, 5, 13]. This skeleton is related to a *discrete structuring element* B, which replaces the disk used in the continuous case. Thus, the discrete skeleton is defined as follows:

MAXIMAL STRUCTURING ELEMENT. If $(nB)_z$ represents the subset obtained after dilating B n-times and shifting the result by z, then the element $(nB)_z$ is maximal if and only if it is included in X and there is no other element $(mB)_y$, $m > n$, such that $(nB)_z \subset (mB)_y \subset X$ [1, 5].

SKELETON IN Z^2. The skeleton $SK^B(X)$ of a set $X \subset Z^2$ is defined as the family of centers z of all maximal structuring elements $(nB)_z$ in X [5].

Lantuejoul [13] (see also [1, 2, 5]) proved that the skeleton can be computed via basic morphological operations. Before introducing the *modified morphological skeleton*, we first present the discrete version of Lantuejoul's algorithm, as used by Maragos and Schafer in [5] for binary image coding. Assume X to be a discrete set, and B a discrete structuring element (i.e., sets in Z^2), then the skeleton $SK^B(X)$ is given by [1, 5].

$$SK^B(X) = \bigcup_{n=0}^{N(B)} S_n^B(X), \tag{10}$$

where

$$S_n^B(X) = (X \ominus nB) - (X \ominus nB) \circ B \tag{11a}$$

$$n = 0, 1, \ldots, N(B) \tag{11b}$$

$$N(B) = \max \{n: X \ominus nB \neq \varnothing\}. \tag{11c}$$

The subset $S_n^B(X)$ is called the nth skeleton subset of X, computed with the structuring element B. The nth skeleton subset $S_n^B(X)$ contains all the points $z \in X$ (and only those points) such that the element $(nB)_z$ is maximal in X [5]. Therefore, $SK^B(X)$, which is computed with the *fixed* structuring element B, contains all the centers z of maximal structuring elements $(nB)_z$, $n = 0, 1, \ldots, N(B)$.

Opened versions of X can be obtained via

$$X \circ kB = \bigcup_{n=k}^{N(B)} S_n^B(X) \oplus nB, \tag{12}$$

where $0 \leq k \leq N(B)$. Hence, if $k = 0$ the original image is reconstructed.

Maragos and Schafer [5] pointed out some of the most important properties of the discrete morphological skeleton together with a very efficient algorithm for computing it.

B. Modified Morphological Skeleton

The morphological skeleton just presented is computed via the structuring element B, having a fixed shape, but linearly increasing in size (as nB is used in equations (11) and (12)). We describe next a morphological skeleton, for which the size of the structuring element increases exponentially by *doubling* its size with each subsequent skeleton step (n). I.e., the size of the structuring element in step $n + 1$ of the skeleton computation is twice as big as the size of the one used in step n (the shape remains unchanged). This representation is motivated by the fact that when larger structuring elements are used, fewer skeleton subsets are obtained (Eq. (11c)), making possible in this way a higher compression ratio (see next section). In the modified morphological skeleton of X, each skeleton subset is computed with the largest possible structuring element; i.e., an element kB such that if $Y = X \circ kB$, then $Y \circ kB = Y$ and $Y \circ (k+1)B \subseteq Y$. Note that in this case, $S_0^{kB}(Y) = \varnothing$, but $S_0^{(k+1)B}(Y) \neq \varnothing$, where $S_0^{mB}(W)$ stands for the set of skeleton points whose contribution via their corresponding maximal structuring element is less than mB (those are skeleton points of "radius zero," see Eq. (11)). From Eq. (12) we get

$$X = X \circ B + S_0^B(X) \tag{13}$$

and

$$X \circ B = \bigcup_{n=1}^{N(B)} S_n^B(X) \oplus nB \tag{14}$$

$$= \bigcup_{n=2}^{N(B)} S_n^B(X) \oplus nB + S_1^B(X) \oplus B,$$

therefore

$$X \circ B = X \circ 2B + S_1^B(X) \oplus B. \tag{15}$$

Now, from Eqs. (10)–(12), we can decompose $X \circ 2B$ in a different way,

$$X \circ 2B = \bigcup_{n=1}^{N(2B)} S_n^{2B}(X) \oplus n2B \qquad (16)$$
$$= X \circ 4B + S_1^{2B}(X) \oplus 2B,$$

Where $S_n^{2B}(X)$, $n = 1, 2, \ldots, N(2B)$, are the skeleton subsets of X computed with the structuring element $2B$ (instead of continuing the computation with the structuring element B). Note that the union goes from $n = 1$ due to the use of $2B$ as the structuring element in the skeleton computation of the set $X \circ 2B$ (if a larger structuring element $-kB$, $k > 2$, is attempted, it could not guarantee that $S_0^{kB}(X \circ 2B) = \varnothing$).
Using Eqs. (13)–(16) we can therefore write

$$X = X \circ 4B + S_1^{2B}(X) \oplus 2B + S_1^{B}(X) \oplus B + S_0^{B}(X). \qquad (17)$$

Subsequently, $X \circ 4B$ can be decomposed using $4B$ as a structuring element (Eqs. (10)–(12)), and this procedure can be continued by *doubling* the size of the structuring element at each step. We obtain this way the *modified morphological skeleton* $MS(X)$ [6, 14],

$$MS(X) = \bigcup_{n=0}^{N_M(B)} M_n(X), \qquad (18)$$

where

$$M_0(X) = S_0^B(X) \qquad (19a)$$
$$M_n(X) = S_1^{B(n)}(X), \qquad n = 1, \ldots, N_M(B) \qquad (19b)$$
$$B(n) \triangleq 2^{n-1}B, \qquad n = 1, \ldots, N_M(B) \qquad (19c)$$
$$N_M(B) = \max\{n: X \ominus 2^{n-1}B \neq \varnothing\}. \qquad (19d)$$

The skeleton subset $M_n(X)$ ($n \geq 1$) contains all the points $z \in X$ (and only those points) such that the element $(2^{n-1}B)_z$ is maximal in X. Therefore, $MS(X)$ contains all the centers z of maximal structuring elements $(2^{n-1}B)_z$, $n = 1, 2, \ldots, N_M(B)$, as well as the subset $M_0(X)$ which contains skeleton points of "radius zero." We observe that with this modified morphological skeleton, fewer skeleton subsets are obtained due to the use of an exponentially increasing size structuring element, since $N_M(B) = \lceil \log_2 N(B) \rceil < N(B)$.

The image can be reconstructed from the modified morphological skeleton as

$$X \circ B(k) = \bigcup_{n=k}^{N_M(B)} [M_n(X) \oplus B(n)], \qquad (20)$$

where $0 \leq k \leq N_M(B)$. Hence, for $k = 0$ with $B(0) \triangleq \{(0, 0)\}$, the original image is reconstructed.

As pointed out in the introduction, the *modified* morphological skeleton is found to be a special case of the geometric-step morphological skeleton (*GSMS*) presented in [8]. It is also possible to derive it from the general morphological representation presented in [15] (see [14]). The motivation for deriving the modified morphological skeleton, as explained at the beginning of this section, is quite different from the motivation for deriving the *GSMS*, resulting in a different, more specific, development method. Thus, in addition to the computational advantage of the *modified* morphological skeleton, as reported in [8], it has an advantage in coding as presented here.

V. GRAY-LEVEL IMAGE CODING

Figure 5 presents the block diagram of the coding algorithm. We next describe each of the coder stages.

A. *Preprocessing*

The aim in using the preprocessing stage is to represent the original image in a form which is more appropriate for our coding method.

The first step in this stage reduces the number of bit planes via the Floyd–Steinberg error diffusion algorithm [9]. We found that when an 8-bit image is reduced to a 4-bit one with this method, a reasonably good quality image is obtained (in contrast with the poor quality obtained by simple truncation). The image can be reduced to a different number of bit-planes, depending on the desired quality and bit-rate, but 4 bits were found to provide a good compromise. With this technique we eliminate the least significant bit-planes of the 8-bit image, which due to their random-like structure, are typically difficult to compress. Thus, using 4 bit-planes with error diffusion, the compression ratio is increased with no significant degradation. Subsequently, pixels in these 4 bit-planes are represented in Gray-code, obtaining more uniform bit-planes which improves the coding algorithm performance.

The original image can also be prefiltered with a two-dimensional 3×3 median filter or with a morphological filter before the error diffusion step. On the basis of the Human Visual System properties [16, 17], such filters improve the coder performance without significant changes in visual quality (see experimental results section).

B. *Bit-Plane Representation*

Each one of the four bit-planes obtained after the preprocessing stage is represented by the modified morphological skeleton described in the previous section (Eqs. (18)–(20)). The bit-planes' geometric structure is very

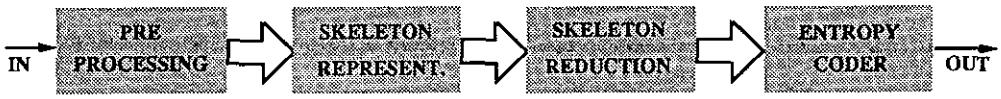

FIG. 5. Block diagram of the proposed morphological image coding algorithm.

general and no preference for any special structuring element can be pointed out a priori. Therefore, we used a 3 × 3 square as the basic structuring element (B) which is related to an 8-cell-neighborhood and is very frequently used in morphological skeleton algorithms [1, 5, 11]. Usually, no more than 6 skeleton subsets were obtained for the different bit-planes ($N_M(B) = 5$, see Eqs. (18) and (19d)).

C. Skeleton Reduction

The morphological skeleton (as well as the *modified morphological skeleton*) is a redundant representation, since some skeleton points can be removed and exact reconstruction of the image from the reduced morphological skeleton can still be obtained. Maragos and Schafer [5] pointed this out and proposed an algorithm for eliminating redundant skeleton points. However, their algorithm does not always find the *minimal* possible number of skeleton points which still allows reconstruction. Our approach to removing redundant skeleton points is based on their algorithm but is improved by using results from the Geometric Sampling Theorem proved in Section III.

Essential points of a *discrete* skeleton can be defined in a similar way to the essential points of a continuous skeleton:

DISCRETE ESSENTIAL POINT. A skeleton point s, $s \in MS(X)$, $X \subset Z^2$, is a *discrete essential point* if and only if there exists a point p in X such that the maximal element corresponding to s is the only one which contains it.

Discrete essential points can be found via a "voting process" similar to the one used in [5] for the calculation of minimal skeletons: For each subset n, a binary function $k_n(i, j)$, whose value is equal to one at points $(i, j) \in B(n)$ and zero everywhere else, is created. This function is called the *characteristic function* of the set $B(n)$ [5]. Then, for each n, k_n is shifted to all points of $M_n(X)$. The contributions of the shifted k_n are added algebraically for all the points of $M_n(X)$ and for all n, obtaining a multivalued function $f(X)$. In order to check if a skeleton point $(r, t) \in M_n(X)$ is essential or not, we check if the value of $f(X)$ at one of the positions given by the characteristic function k_n shifted to (r, t) (i.e., $k_n(i - r, j - t)$), is equal to one. If the answer is positive, that skeleton point is essential. If all the values are ≥ 2, then that skeleton point is not essential.

Computation of the multivalued function $f(X)$ requires one pass through all skeleton points [5]. Searching for the essential points requires a second pass through skeleton points. In contrast with the algorithm presented in [5] for minimal skeleton computation, the function $f(X)$ is not altered during the second pass (reducing the algorithm complexity), and the result does not depend on the scan order (since the set of essential points is unique by definition). Also, for storing the function $f(X)$, just two bits are needed, since in order to decide whether a skeleton point is essential or not, one needs to know only if $f(X)$ is equal to zero, one, or greater than one (in [5], the exact value of $f(X)$ is needed).

Simulation results show that the discrete essential points constitute only about 10% of all skeleton points.

A dual Geometric Sampling Theorem for discrete images is not known; i.e., a theorem which relates the *discrete* minimal reconstruction X^* (defined as in the continuous case) to the discrete set X is not known. However, we found that the essential points of a discrete skeleton do reconstruct most of the image (typically close to 90%). Therefore, the set of essential points is almost sufficient, and we have to care only about the "optimal" coverage of a small part of the image (typically 10%) instead of the "optimal" coverage of the whole image as in [5]. Thus, after the essential points are found, the resulting *search space* is much smaller than the original one, and a solution closer to the optimal one can be found using simpler methods. We decided to select the additional skeleton points (i.e., those needed in addition to the essential points) according to the contributions of their corresponding maximal element to the partial reconstructed image (see Eqns. (6), (12), and (20)). We denote by $M'_n(X)$ the reduced skeleton subset obtained from the essential points of $M_n(X)$ and the additional nonessential points that were added, as explained above, for exact reconstruction. Then, $M'_n(X) \subseteq M_n(X)$, and typically Card $[M'_n(X)] \ll$ Card $[M_n(X)]$ (Card $[\cdot]$ stands for the cardinality of the set). Hence, each of the bit-planes is completely represented (i.e., error-free) by its *reduced modified morphological skeleton* (*RMMS*):

$$RMMS(X) = \bigcup_{n=0}^{N_M(B)} M'_n(X) \tag{21}$$

$$X = \bigcup_{n=0}^{N_M(B)} M'_n(X) \oplus B(n). \tag{22}$$

Opening versions can be obtained in a form similar to Eq. (20).

Before proceeding with coding the *RMMS*, we point out that simulation results suggest that a discrete version of Theorem 1 may be valid. Therefore, when checking if a skeleton point is essential or not, it appears to be enough to check the contribution of its maximal element to the boundary, thereby reducing the computational complexity of the presented skeleton reduction approach (this complexity is *linear* in the maximal structuring element size instead of *quadratic* as in [5]).

D. RMMS Coding

Each skeleton subset $M'_n(X)$ of the *RMMS* bit-plane representation is coded as a full size binary image (which is generally very sparse). Such an image has a value of one at (i,j) if (i,j) is a point in $M'_n(X)$, and a value of zero everywhere else. These binary images are coded one after the other, in an decreasing (or increasing) order of n. Giving an apriori order, no coding of the size of $B(n)$ is needed. Better compression ratios were obtained when coding the *RMMS* this way instead of coding it as a multilevel image, where the level indicates the corresponding radius. Coding the *RMMS* as a set of binary images is also more appropriate for bit-plane coding when geometric errors are introduced (see next).

Two different entropy coding schemes are used: one for coding lines in the binary images (which represent skeleton subsets) having no skeleton points (empty lines), and another for the remaining lines. First, a Huffman code for the number of consecutive empty lines is generated, by which the exact position of nonempty lines can be pointed out. The position of each skeleton point in its corresponding nonempty line is then coded by run-length and Huffman coding.

This coding strategy was found to be very efficient for *RMMS* coding, because of their special structure as mentioned above. An improvement in the compression ratio was obtained using the *RMMS* representation instead of the original morphological skeleton representation proposed by Maragos and Schafer [5], mainly due to the reduction in the number of skeleton subsets (see next section for compression results).

By introducing geometric errors in the different bit-planes, the compression ratio can be increased. These errors correspond to the omission of *RMMS* subsets $M'_n(X)$, $n < r \leq N_M(B) + 1$, where r is selected according to the bit-plane importance (for more significant bit-planes, r is small or even zero, i.e., no *RMMS* subsets are omitted); obtaining with this method smoothed versions of the form $X \circ B(r)$ of the bit-planes (equation (20)). If just the smoothed bit-plane were coded, missing points of X ($X \circ B(r) \subseteq X$) would appear in the reconstruction as part of the background. This could cause considerable degradation of the subjective image quality. To circumvent this problem, we coded the smoothed versions of both X and its complement, X^c, (i.e., both $RMMS(X)$ and $RMMS(X^c)$ are computed and coded), and subsequently fill-in randomly the undefined regions or "holes" (Fig. 6).

VI. SIMULATION RESULTS

To evaluate the performance of the proposed coding scheme, it was simulated on a Vax Station 3200, which is hosting a Gould IP8500 image processing and display system. Since the techniques used in the proposed algorithm (e.g., error-diffusion) are not based on energy minimization (in contrast to transform coding [18]), the performance is evaluated only on the basis of subjective quality of the images, i.e., what the image "looks like" to the observer [16, 17] (see Conclusions).

In the results presented below, an error-free transmission channel or storage media is assumed.

A woman's head and shoulder image ("Lena") of size 512×512 pixels is presented as the first test image (for more examples see below and [14]). Figure 6a shows the original image. Figure 6b shows the image represented using only four bit-planes with error-diffusion. This image was coded (using the *RMMS*) at the rate of 2.0 bits per pixel (b/p), and represents what we call the "four-bit error-free image." Figure 6c shows an image that was initially filtered with a 3×3 median filter followed by 4-bit error-diffusion. This image was coded at 1.7 b/p. The same picture, when represented via the morphological skeleton proposed in [5] (instead of the *RMMS*) is coded at the rate of 1.9 b/p. Figure 6d shows the reconstruction of an image in which the least significant bit-plane (of the 4-bit error-diffusion representation) was coded without skeleton points of radius zero; both the image and the background were coded and "holes" were filled-in randomly (the remaining three bit-planes were coded error-free). This image required 1.5 b/p (as compared with the rate of 2.0 b/p for the image in Fig. 6b).

The second test image is a satellite image. Figure 7a shows the original image. Figure 7b shows the image represented using only four bit-planes with error-diffusion. This image was coded (using the *RMMS*) at the rate of 0.92 b/p. Figure 7c shows an image that was initially filtered with a 3×3 median filter followed by 4-bit error-diffusion. This image was coded at 0.72 b/p.

From our simulation results we conclude that for simple binary images, like the most significant bit-plane (MSB) of a gray-level image, the morphological step in the coding scheme reduces the bit rate (see also [5]). For example, in the case of the most significant bit-plane of the satellite image, the bit-rate is reduced by 50% (from 0.018 b/p to 0.009 b/p). For the well known standard picture "House," this reduction is 16% (from 0.19 b/p to 0.16 b/p).

For more complicated images, such as the least significant bit-planes (LSB), the morphological representation

FIG. 6. Simulation results for "Lena": (a) original image (8 bits); (b) "four-bit error-free image": 2.0 b/p; (c) median-filtered four-bit image: 1.7 b/p; (d) four-bit image with the least significant bit-plane coded after opening by B: 1.5 b/p.

in the coding scheme adds flexibility to the algorithm. In this case, in order to reduce the bit-rate and to achieve also coding advantages from the morphological step, geometric errors should be introduced as explained in the previous section. These errors reduce the total bit-rate by about 20% for the satellite image (in comparison with the bit-rate obtained without the morphological step).

Since each bit-plane is coded in an independent form, the morphological step can be incorporated for the most significant bit-planes only and can be omitted for the others.

VII. SUMMARY AND CONCLUSIONS

In this paper, a new approach for gray-level image coding which uses simple binary morphological operations is presented. This approach is based on bit-plane coding via a new morphological representation derived from a *Geometric Sampling Theorem* and a *modified* morphological skeleton.

The Geometric Sampling Theorem (GST) deals with the reconstruction of the boundary of a *continuous* two-level image from a *unique* subset of points of its skeleton

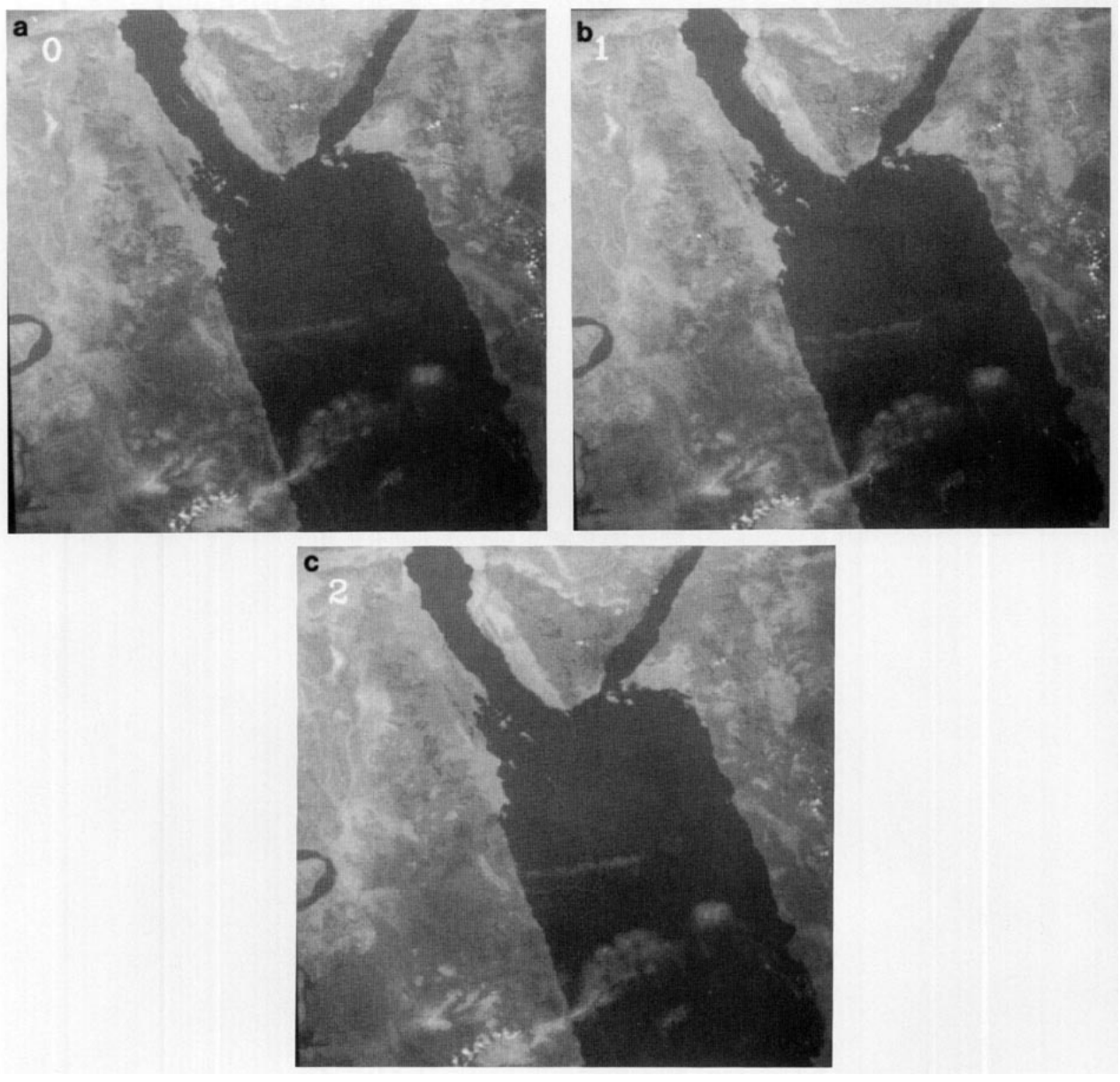

FIG. 7. Simulation results for satellite image: (a) original image (8 bits); (b) "four-bit error-free image": 0.92 b/p; (c) median-filtered four-bit image: 0.72 b/p.

representation. This set of points, called *essential points*, was found to play an important role in the skeleton representation of *discrete* binary-image as well. Based on this fact, an efficient algorithm for morphological skeleton reduction is proposed.

A *modified morphological skeleton* for binary image representation is also described. This skeleton is computed with an *exponentially increasing in size* structuring element. In this way, the number of skeleton subsets is reduced (which was the motivation for developing this representation), resulting in an increased compression ratio. While the computational advantage of this representation is pointed out in [8], here we demonstrate its advantage in efficient representation for coding applications.

In the second part of the paper, details of the proposed morphological image coder are presented. The main steps are as follows: The image is first reduced from 8 bits to 4 bits via an error-diffusion algorithm, and the pixels are subsequently converted to Gray-code. The resulting bit-planes are represented via the *modified morphological skeleton*. Redundancy in the representation is then reduced via an algorithm which is based on the *GST*. An entropy coding scheme, particularly devised for efficient

coding of these skeletons, is the last step. The possibility of reduction of the bit rate by the introduction of geometric errors is also demonstrated.

The proposed coding scheme can be considered as a step in the direction of geometric coding of gray-level images. It is quite different from morphological coding approaches which are based on image segmentation and labeling (e.g., [19]). It is also found that the error introduced by geometric deformations is, in general, more acceptable to the observer than the blocking or quantization errors introduced by standard image coding algorithms.

This work points to several open problems: First, finding a morphological skeleton which allows a structuring element with changing *shape* (not just *size*, see [19, 20]) may further improve the compression ratio. Second, the introduction of geometric errors directly in the gray-level image (and not just through the bit planes) could be more beneficial and should be investigated.

APPENDIX

The next theorem gives a lower bound on the length of the skeleton arcs eliminated when opening a continuous set with a continuous disk (see Section III.B):

THEOREM 3. *If* $Y_\rho \neq Y_{\rho+r}$, *then* $L[\Psi(Y_\rho)] - L[\Psi(Y_{\rho+r})] \geq r$, *where* $L(\cdot)$ *stands for arc length.*

Proof. If we define $\sigma_P(p)$ as the Euclidean distance of a point p in a set $P \leq R^2$ to the set boundary ∂P, then $\sigma_P(\cdot)$ is a Lipshitz function [2, Chap. 11]; i.e., $|\sigma_P(p) - \sigma_P(q)| \leq d(p, q)\ \forall\ p, q \in P$ ($d(\cdot, \cdot)$ is the Euclidean distance in R^2). In the case where p, q are skeleton points, i.e., $p, q \in \Psi(P)$, $|\sigma_P(p) - \sigma_P(q)| < d(p, q)$ [2, Chap. 11].

Let y be one of the skeleton points of Y_ρ, $y \in \Psi(Y_\rho)$, with correspondent skeleton radius ρ (such a point exists from the hypothesis and Eq. (6), i.e., $\sigma_{Y_\rho}(y) = \rho$). Travel from y a distance r through the skeleton in a given direction (if this is not possible, the skeleton length is less than $2r$, which is not an important case). Call this arc Δ ($\Delta \subseteq \Psi(Y_\rho)$). For any point $z \in \Delta$, we have

$$\sigma_{Y_\rho}(z) - \sigma_{Y_\rho}(y) < d(y, z) \leq r,$$

then

$$\sigma_{Y_\rho}(z) < \sigma_{Y_\rho}(y) + r = \rho + r,$$

and therefore z is eliminated by opening with the element $(\rho + r)B$. Hence, the whole segment Δ, of length $L(\Delta) = r$, is eliminated. ■

The number of eliminated disjoint arcs Δ of length r depends on the number of points y in Y_ρ having $\sigma_{Y_\rho}(y) = \rho$, and on the distance between them [14].

ACKNOWLEDGMENTS

The authors thank the anonymous reviewers for their useful comments, and Renato Kresch for useful discussions and assistance in preparing the simulations.

REFERENCES

1. J. Serra, *Image Analysis and Mathematical Morphology*, Vol. 1, Academic Press, New York, 1982.
2. J. Serra (Ed.), *Image Analysis and Mathematical Morphology*, Volume 2: Theoretical Advances, Academic Press, New York, 1988.
3. H. Blum, Biological shape and visual science, *J. Theoret. Biol.* **38,** 1973, 205–287.
4. L. Calabi and W. E. Hartnett, Shape recognition, prairie fires, convex deficiencies and skeletons, *Amer. Math. Monthly* **75,** 1968, 335–342.
5. P. A. Maragos and R. W. Schafer, Morphological Skeleton Representation and Coding of Binary Images, *IEEE Trans. Acoust. Speech, Signal Process.* **ASSP-34** (5), 1986, 1228–1244.
6. G. Sapiro and D. Malah, A geometric sampling theorem and its application in morphological image coding, in *Proceedings of the International Conference on Digital Signal Processing, Florence, September 1991.*
7. G. Sapiro and D. Malah, Morphological image coding via bit-plane decomposition and a new skeleton representation, in *Proceedings of the 17th IEEE Convention of Electrical and Electronics Engineers in Israel, May 1991.*
8. D. Schonfeld and J. Goutsias, A fast algorithm for the morphological coding of binary images, in *Visual Communication and Image Processing '88, Proc. SPIE* **1001,** 1988, 138–145.
9. R. Ulichney, *Digital Halftoning*, MIT Press, Cambridge, MA, 1987.
10. C. R. Giardina and E. R. Dougherty, *Morphological Methods in Image and Signal Processing*, Prentice–Hall, Englewood Cliffs, NJ, 1987.
11. R. M. Haralick, S. R. Stenberg, and X. Zhuang, Image analysis using mathematical morphology, *IEEE Trans. Pattern Anal. Mach. Intelligence* **PAMI-9,** 1987, 532–550.
12. M. P. Do Carmo, *Differential Geometry of Curves and Surfaces*, Prentice–Hall, Englewood Cliffs, NJ, 1976.
13. C. Lantuejoul, *La squelettisation et son application aux mesures topologiques des mosaiques polycristallines*, These de Docteur-Ingenieur, School of Mines, Paris, France, 1978.
14. G. Sapiro, *Image Coding via Morphological Techniques*, M.Sc. Thesis, Department of Electrical Engineering, Technion—Israel Institute of Technology, 1991. [In Hebrew]
15. J. Goutsias and D. Schonfeld, Morphological representation of discrete and binary images, *IEEE Trans. Signal Proc.* **39** (6), 1991, 1369–1379.
16. M. Kunt, A. Ikonomopolous, and M. Kocher, Second generation image-coding techniques, *Proc. IEEE* **73,** 1985, 549–574.
17. S. A. Rajala, H. A. Peterson, and E. J. Delp, Binary morphological coding of gray-scale images, in *Proceedings of the IEEE International Symposium on Circuits and Systems—ISCAS '88*, pp. 2807–2811.

18. A. Rosenfeld and A. C. Kak, *Digital Picture Processing*, Academic Press, New York, 1982.
19. P. Maragos, Morphology-based symbolic image modeling, multiscale nonlinear smoothing, and pattern spectrum, in *Proceedings of the IEEE Conference on Computer Vision and Pattern Recognition—CVPR '88, Ann Arbor, MI, 1988*, pp. 766–773.
20. C. Ronse and B. Macq, *Morphological Shape and Region Description*, Internal Report, Philips Research Laboratory Belgium, January 1991.

GUILLERMO SAPIRO was born in Montevideo, Uruguay, on April 3, 1966. He received the B.Sc. degree (suma cum laude) in computer engineering and the M.Sc. in electrical engineering, both from the Technion—Israel Institute of Technology, Haifa, Israel, in 1989 and 1991 respectively. He is currently working toward the D.Sc. degree in the Department of Electrical Engineering at the Technion. Since 1989 he has been a teaching assistant at the Technion and an undergraduate students project supervisor at the Signal Processing Laboratory of the Electrical Engineering Department. His research interests are in the area of curve evolution theory, image processing, and computer vision. G. Sapiro was awarded the Gutwirth Scholarship for Special Excellence in Graduate Studies in 1991.

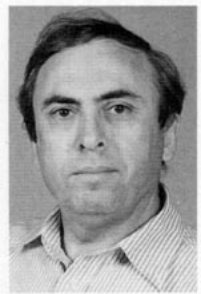

DAVID MALAH received the B.Sc. and M.Sc. degrees in 1964 and 1967, respectively, from the Technion—Israel Institute of Technology, Haifa, Israel, and the Ph.D. degree in 1971 from the University of Minnesota, Minneapolis, Minnesota, all in electrical engineering. During 1971–1972 he was an assistant professor at the Electrical Engineering Department of the University of New Brunswick, Fredericton, New Brunswick. In 1972 he joined the Electrical Engineering Department of the Technion, where he is presently a professor. From 1979 to 1981 he was on sabbatical and leave at the Acoustic Research Department of AT&T Bell Laboratories, Murray Hill, New Jersey, and a consultant at Bell Labs during the summers of 1983, 1986, 1988, and 1991. During 1988–1989 he was on sabbatical leave at the Signal Processing Research Department of AT&T Bell Laboratories in Murray Hill. Since 1975 (except during 1979–1981 and 1988–1989) he has been in charge of the Signal Processing Laboratory at the Electrical Engineering Department which is active in speech and image communication research and real-time hardware development. His main research interests are in image and speech coding, image and speech enhancement, and digital signal processing techniques. Since 1987 he has been a fellow of the IEEE.